Available online at www.sciencedirect.com
ScienceDirect
International Journal of Heat and Mass Transfer 51 (2008) 1085–1094
International Journal of HEAT and MASS TRANSFER
www.elsevier.com/locate/ijhmt

Mixed convection heat transfer in inclined rectangular ducts with radiation effects

Han-Chieh Chiu [a], Wei-Mon Yan [b,*]

[a] Department of Mechanical Engineering, Technology and Science of Northern Taiwan, Pei-To, Taipei, Taiwan 112, Taiwan, ROC
[b] Department of Mechatronic Engineering, Huafan University, Shih Ting, Taipei, Taiwan 223, Taiwan, ROC

Received 14 February 2007; received in revised form 23 May 2007
Available online 26 July 2007

Abstract

A numerical study was carried out to investigate the radiation effect on the characteristics of the mixed convection fluid flow and heat transfer in inclined ducts. The three-dimensional Navier–Stokes equations and energy equation are solved simultaneously with the vorticity–velocity method. The integro-differential radiative transfer equation was solved by the discrete ordinates method. The effects of the thermal buoyancy and the radiative transfer on the distributions of the bulk fluid temperature, the friction factor and the Nusselt number are emphasized in detail. Results indicate that radiation effects have a considerable impact on the heat transfer and tend to reduce the thermal buoyancy effects. In addition, the development of the bulk fluid temperature is enhanced by the radiation effects.

Keywords: Mixed convection; Inclined rectangular ducts; Radiation effects

1. Introduction

There are many thermal engineering applications involving thermal radiation with combined buoyancy and forced convection. Heat exchangers, furnace design, thermal insulation, electronic system, and cooling processes in nuclear reactors are some examples. In general, heat transfer resulting from coupled processes cannot be calculated separately in such systems. Otherwise, significant error would occur due to the interaction between convection and thermal radiation. Considering the flowing medium as a radiating molecular gas, its complex absorption and emission spectra introduce an important difficulty in the simulation of these flows. Therefore, most of the previous studies on combined thermal radiation and mixed convection are based on simplifying assumptions such as gray gases [1].

There have been various studies of the analysis of the combined radiation and convection modes of heat transfer [2–12]. Forced convection in a channel with radiation has been under investigation by many researchers [2–5] for ducts with prescribed heat fluxes and temperature distributions on wall surface. Various approximate methods have been employed for radiative transport in the medium in these studies. Besides, the differential approximation methods describe approximation variation of the intensity of radiation as a function of position and angle. In recent years, heat transfer by simultaneous free or mixed convection and radiation has been studied [6–10]. However, some of the studies are focused on the micropolar fluid [11,12], while some of the studies pay attention on the porous boundary [13,14]. Recently, Debbissi et al. [15] studied evaporation of water in a vertical channel including effects of wall radiation. Sediki et al. [16] investigated the interaction between radiation and mixed convection for ascending flows in vertical circular tubes.

For internal flows of mixed convection heat transfer, the interactions of hydrodynamic and thermal development become fairly complicated. Many works have been done on mixed heat transfer in laminar or turbulent flows in vertical and horizontal rectangular ducts [17–23].

* Corresponding author.
E-mail address: wmyan@huafan.hfu.edu.tw (W.-M. Yan).

0017-9310/$ - see front matter © 2007 Elsevier Ltd. All rights reserved.
doi:10.1016/j.ijheatmasstransfer.2007.05.009

Nomenclature

A	cross-sectional area of inclined rectangular ducts (m^2)
a, b	width and height of inclined rectangular ducts, respectively (m)
c_p	specific heat ($J\,kg^{-1}K^{-1}$)
D_e	equivalent hydraulic diameter, $2ab/(a+b)$
f	friction factor, $2\tau_w/(\rho_o w_o^2)$
G,G^*	dimensional and dimensionless incident radiation, $G^* = \frac{G}{(4\bar{n}^2\sigma T_w^4)}$
Gr	Grashof number, $g\beta(T_w - T_o)D_e^3/v^2$
$\bar{h}$	circumferentially average heat transfer coefficient ($W\,m^{-2}\,K^{-1}$)
k	thermal conductivity ($W\,m^{-1}\,K^{-1}$)
m, m'	direction of the discrete ordinates
M, N	number of the finite difference divisions in the X and Y directions, respectively
n	direction coordinate normal to the duct wall
$\bar{n}$	refractive index
N^*	order of phase function
N_c	conduction-to-radiation parameter, $k\kappa/(4\bar{n}^2\sigma T_w^4)$
Nu_c	local convective Nusselt number
Nu_r	local radiative Nusselt number
Nu_t	local total Nusselt number
$\bar{p}$	cross-sectional mean pressure (kPa)
$\bar{P}$	dimensionless cross-sectional mean pressure
p'	perturbation term about mean pressure (kPa)
P'	dimensionless perturbation pressure
Pe	Peclet number, $Pr \cdot Re$
P_n	Legendre polynomial
Pr	Prandtl number, v/α
Q_r	dimensionless radiation flux
$\vec{q}_c$	convective heat flux (Wm^{-2})
$\vec{q}_r$	radiative heat flux (Wm^{-2})
$\vec{q}_t$	total heat flux (Wm^{-2})
Ra	Rayleigh number, $Pr \cdot Gr$
Ra^*	$Ra \times \cos\Theta$
Re	Reynolds number, $w_o D_e/v$
s	perimeter of duct cross-section, $2(a+b)$
T	temperature (K)
T_o	inlet temperature (K)
U, V, W	dimensionless velocity components in the X, Y, and Z directions, respectively
u, v, w	velocity components in the x, y, and z directions, respectively ($m\,s^{-1}$)
w_o	uniform velocity at the inlet, m/s
X, Y, Z	dimensionless rectangular coordinate, $X = x/D_e$, $Y = y/D_e$, $Z = z/(D_e \cdot Re)$
Z^*	dimensionless z-direction coordinate, $z/(Pr \cdot Re \cdot D_e) = Z/Pr$
x, y, z	rectangular coordinate system (m)

Greek symbols

α	thermal diffusivity ($m^2\,s^{-1}$)
β	coefficient of thermal expansion (1/°K)
$\bar{\beta}$	extinction coefficient, m^{-1}
γ	aspect ratio of a rectangular duct, b/a
δ	mixed convection parameter
ε_w	wall emissivity
ϕ	scattering phase function
κ_s	scattering coefficient, m^{-1}
θ	dimensionless temperature, T/T_w
θ_o	dimensionless inlet temperature, T_o/T_w
Θ	inclination angle
μ, η, ζ	direction cosines
v	kinematic viscosity ($m^2\,s^{-1}$)
ρ	density ($kg\,m^{-3}$)
σ	Stefan–Boltzman constant, 5.67×10^{-8} W/$m^2\,K^{-4}$
τ	optical thickness
τ_w	wall shear stress, kPa
$\underline{\omega}$	single scattering albedo
$\vec{\Omega}, \vec{\Omega}'$	outward and inward direction of radiation
ξ	dimensionless vorticity in the axial direction, $\partial U/\partial Y - \partial V/\partial X$
ψ	dimensionless radiation intensity, $\pi I/(\bar{n}^2\sigma T_w^4)$

Superscript

$\bar{}$	mean quantity

Subscripts

b	bulk fluid quantity
c	convective
o	condition at inlet
r	radiative
w	value at wall

However, different orientations of the channel can induce different kinds of heat buoyant flows which enhance the heat transfer in different manners. For inclined ducts, buoyancy forces act in both main flow and the cross-stream directions. In fact, the buoyancy forces can be decomposed into two components: one normal to and another parallel with the forced flow. Huang and Lin [24] investigated the transient mixed convection air flow in a bottom heated inclined rectangular duct. Their attention was particularly paid to delineate the effects of the duct inclination on the flow transition with heat transfer only.

It is noted from the paper review cited above that studies of simultaneous effect of thermal buoyancy and radiation in inclined duct flows have never been investigated. This motivates the present study. The purpose of this study is

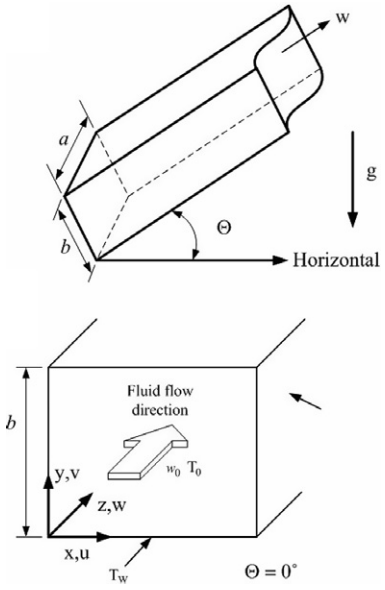

Fig. 1. Schematic diagram of the physical system.

to investigate the laminar mixed convection and thermal radiation in inclined rectangular ducts.

2. Analysis

A rectangular duct with inclination angle Θ, width a, and height b is considered as shown in Fig. 1. To focus the radiation effects, the entering upward flow is assumed to be steady and laminar. A uniform axial velocity w_o and a constant temperature T_o are imposed at the inlet ($z = 0$). The velocity components in x, y, and z directions are denoted as u, v, and w, respectively. The thermophysical properties of the fluid are taken to be constant except for the density variation in the buoyancy terms of the y- and z-direction momentum equations. The Boussinesq approximation is employed for the thermal buoyancy effect. The viscous dissipations and compression effect in the energy equation are neglected due to low Mach number flows. The walls are maintained at a uniform constant temperature, T_w. In addition, the gas is assumed to be gray, emitting, absorbing, and scattering. The flow is considered to be parabolic for this study. In the momentum equations, a space-averaged pressure $\bar{p}$ is imposed to prevail at each cross-section, permitting a decoupling of the pressure in the cross-sectional momentum equation. Together with the neglect of axial diffusion of momentum and heat, the dynamic pressure p_m can then be presented as the sum of a cross-sectional mean pressure, $\bar{p}(z)$, which drives the main flow, and a perturbed pressure about the mean, $p'(x, y, z)$, which drives the cross-stream flow,

$$p_m = \bar{p}(z) + p'(x, y, z) \tag{1}$$

For systematical analysis, the dimensionless groups are introduced as:

$$X = x/De, \quad Y = y/De, \quad Z = z/(De \cdot Re), \quad De = 4A/s$$
$$Z^* = Z/Pr, \quad U = uDe/v, \quad V = vDe/v, \quad W = w/w_o$$
$$\theta_o = T_o/T_w, \quad \theta = T/T_w, \quad \bar{P} = \bar{p}/(\rho_o w^2), \quad P' = p'/(\rho_0 v^2/De^2)$$
$$Pr = v/\alpha, \quad Re = w_o De/v, \quad Ra = Pr \cdot Gr, \quad \gamma = b/a$$
$$Ra^* = Ra \cdot \cos\Theta, \quad \delta = (Ra/Re)\sin\Theta, \quad N_c = k\kappa/(4\bar{n}^2\sigma T_w^4),$$
$$G^* = G/(4\bar{n}^2\sigma T_w^4)$$
$$\tau = \kappa De, \quad Gr = g\beta(T_w - T_o)De^3/v^2, \quad \omega = \kappa_s/\kappa \tag{2}$$

The non-dimensional governing equations of mass, momentum, and energy can be formulated as follows:

Continuity equation

$$\frac{\partial U}{\partial X} + \frac{\partial V}{\partial Y} + \frac{\partial W}{\partial Z} = 0 \tag{3}$$

Momentum equations

$$U\frac{\partial U}{\partial X} + V\frac{\partial U}{\partial Y} + W\frac{\partial U}{\partial Z} = -\frac{\partial P'}{\partial X} + \frac{\partial^2 U}{\partial X^2} + \frac{\partial^2 U}{\partial Y^2} \tag{4}$$

$$U\frac{\partial V}{\partial X} + V\frac{\partial V}{\partial Y} + W\frac{\partial V}{\partial Z} = -\frac{\partial P'}{\partial Y} + \frac{\partial^2 V}{\partial X^2} + \frac{\partial^2 V}{\partial Y^2} + \frac{Ra\cos\Theta}{Pr}\cdot\frac{\theta - \theta_o}{1 - \theta_o} \tag{5}$$

$$U\frac{\partial W}{\partial X} + V\frac{\partial W}{\partial Y} + W\frac{\partial W}{\partial Z} = -\frac{\partial \bar{P}}{\partial Z} + \frac{\partial^2 W}{\partial X^2} + \frac{\partial^2 W}{\partial Y^2} + \frac{Ra\sin\Theta}{Pr\cdot Re}\cdot\frac{\theta - \theta_o}{1 - \theta_o} \tag{6}$$

Energy equation

$$U\frac{\partial \theta}{\partial X} + V\frac{\partial \theta}{\partial Y} + W\frac{\partial \theta}{\partial Z} = \frac{1}{Pr}\left[\frac{\partial^2\theta}{\partial X^2} + \frac{\partial^2\theta}{\partial Y^2} + \frac{(1-\omega)\tau^2}{N_c}\cdot(G^* - \theta^4)\right] \tag{7}$$

The non-dimensional vorticity in axial direction can be expressed as

$$\xi = \partial U/\partial Y - \partial V/\partial X \tag{8}$$

By combining Eq. (8) with (5)–(7), the governing equations can then be derived as follows:

$$U\frac{\partial \xi}{\partial X} + V\frac{\partial \xi}{\partial Y} + W\frac{\partial \xi}{\partial Z} + \xi\left(\frac{\partial U}{\partial X} + \frac{\partial V}{\partial Y}\right) + \left(\frac{\partial W}{\partial Y}\cdot\frac{\partial U}{\partial Z} - \frac{\partial W}{\partial X}\cdot\frac{\partial V}{\partial Z}\right)$$
$$= \frac{\partial^2\xi}{\partial X^2} + \frac{\partial^2\xi}{\partial Y^2} - \frac{(Ra\cos\Theta)}{Pr}\cdot\frac{\partial\theta/\partial X}{1 - \theta_o} \tag{9}$$

$$\frac{\partial^2 U}{\partial X^2} + \frac{\partial^2 U}{\partial Y^2} = \frac{\partial \xi}{\partial Y} - \frac{\partial^2 W}{\partial X \partial Z} \tag{10}$$

$$\frac{\partial^2 V}{\partial X^2} + \frac{\partial^2 V}{\partial Y^2} = -\frac{\partial \xi}{\partial X} - \frac{\partial^2 W}{\partial Y \partial Z} \tag{11}$$

Additional constrain for the mass conservation requires that the mass flow rate at any axial location be the same, hence

$$\int_0^{(1+\gamma)/(2\gamma)}\int_0^{(1+\gamma)/2} W\,dX\,dY = \frac{(1+\gamma)^2}{4\gamma} \tag{12}$$

The pressure gradient in the axial momentum equation can be obtained by employing Eq. (12).

Concerning the radiation transfer, the medium is considered as gray, absorbing and scattering. The dimensionless form of the radiation transfer equation is expressed as

$$\mu\frac{\partial\psi}{\partial X}+\eta\frac{\partial\psi}{\partial Y}+\tau\psi=(1-\omega)\tau\theta^4+\frac{\omega\tau}{4\pi}\int_{\Omega'=4\pi\phi}(\vec{\Omega}',\vec{\Omega})\psi\,\mathrm{d}\,\vec{\Omega}' \tag{13}$$

where ψ is the dimensionless intensity of radiation at a location of (X, Y), which is of the form $\pi I/(\vec{n}^2\sigma T_{\mathrm{w}}^4)$. In the equation, the axial term, $\frac{\partial\psi}{\partial Z}$, is dropped by assuming $\frac{\partial q_{rz}}{\partial Z}<<\frac{\partial q_{rx}}{\partial X}+\frac{\partial q_{ry}}{\partial Y}$. The parameters μ, η, and ζ are the direction cosines for the radiation direction $\vec{\Omega}$. The symbol ϕ is the scattering phase function, which can be expressed in terms of Legendre polynomials as

$$\phi(\vec{\Omega}',\vec{\Omega})=\sum_{n=0}^{N}a_nP_n(\mu'\mu+\eta'\eta+\zeta'\zeta) \tag{14}$$

For a gray, opaque, diffusively emitting, and reflecting surface, the boundary condition is

$$\psi_{\mathrm{w}}\vec{\Omega}=\varepsilon_{\mathrm{w}}+\frac{1-\varepsilon_{\mathrm{w}}}{\pi}\int_{\vec{n}\cdot\vec{\Omega}'<0}|\vec{n}\cdot\vec{\Omega}'|\psi_{\mathrm{w}}(\vec{\Omega}')\,\mathrm{d}\,\vec{\Omega}',$$

$$\vec{n}\cdot\vec{\Omega}>0 \tag{15}$$

where ε_{w} is the wall emissivity, and $\vec{n}$ is the unit normal vector pointing away from the duct wall into the medium.

As long as the dimensionless radiation intensity ψ is known, the dimensionless radiation flux vector and incident radiation are re-determined from their definitions as

$$\vec{Q}_{\mathrm{r}}=\frac{\vec{q}_{\mathrm{r}}}{(4\bar{n}^2\sigma T_{\mathrm{w}}^4)}=\frac{1}{4\pi}\int_{\Omega=4\pi}\vec{\Omega}'\,\psi\,\mathrm{d}\Omega \tag{16}$$

$$G^*=\frac{G}{(4\bar{n}^2\sigma T_{\mathrm{w}}^4)}=\frac{1}{4\pi}\int_{\Omega'=4\pi}\psi\,\mathrm{d}\Omega' \tag{17}$$

The corresponding boundary conditions for this study are:

Entrance ($Z=0$):

$$W=1;\quad U=V=\xi=0;\quad \theta=\theta_{\mathrm{o}} \tag{18}$$

Duct walls:

$$U=V=W=0;\quad \theta=1 \tag{19}$$

The governing equations contain dimensionless parameters δ, Ra^*, γ, and Pr, as defined in Eq. (2). The value of δ is a mixed convection parameter, i.e. the ratio of Raleigh number Ra to the Reynolds number Re, is modified by an inclination angle factor $\sin\Theta$. Besides, $Ra^*=Ra\cos\Theta$ is a modified Rayleigh number. The inclination angle does not appear explicitly with the introduction of the independent parameters δ and Ra^*. Apparently, for a horizontal rectangular duct [23],

$$\Theta=0,\quad \sin\Theta=0,\quad Ra^*=Ra,\quad \delta=0 \tag{20}$$

While for a vertical duct,

$$\Theta=\pi/2,\quad \sin\Theta=1,\quad Ra^*=0,\quad \delta=Ra/Re \tag{21}$$

After obtaining the velocity and temperature fields along the axial direction of the rectangular duct, the determination of local friction factor and Nusselt number is of practical interest for the study of mixed convection heat transfer. According to usual definitions, the expression for the product of the peripherally averaged friction factor and Reynolds number are expressed as

$$fRe=-2\overline{\left.\frac{\partial W}{\partial n}\right|_{\mathrm{wall}}} \tag{22}$$

where the over-bar represents the average around the perimeters.

Energy transport from the duct wall to the gas flow depends on two related factors: the fluid temperature gradient on the wall and the rate of radiative heat exchange. Hence, the local total Nusselt number along the duct wall is defined as

$$Nu_{\mathrm{t}}=\frac{\bar{h}\mathrm{D_e}}{k}=\frac{q_{\mathrm{t}}\mathrm{D_e}}{k(T_{\mathrm{w}}-T_{\mathrm{b}})} \tag{23}$$

where $q_{\mathrm{t}}=q_{\mathrm{c}}+q_{\mathrm{r}}=-\partial T/\partial n+q_{\mathrm{r}}$. The Nu_{t} is the sum of local convective Nusselt number, Nu_{c}, and local radiative Nusselt number, Nu_{r}. They are respectively defined as

$$Nu_{\mathrm{c}}=-\frac{\bar{\partial}\bar{\theta}}{\partial n}\frac{1}{1-\theta_{\mathrm{b}}} \tag{24}$$

and

$$Nu_{\mathrm{r}}=\frac{\tau\bar{Q}_{\mathrm{r}}}{N_{\mathrm{c}}}\frac{1}{1-\theta_{\mathrm{b}}} \tag{25}$$

In the above equations, the bulk fluid temperature θ_{b} is defined as

$$\theta_{\mathrm{b}}=\frac{\int_0^{\frac{1+\gamma}{2\gamma}}\int_0^{\frac{1+\gamma}{2}}\theta\cdot W\,\mathrm{d}X\,\mathrm{d}Y}{\int_0^{\frac{1+\gamma}{2\gamma}}\int_0^{\frac{1+\gamma}{2}}W\,\mathrm{d}X\,\mathrm{d}Y} \tag{26}$$

3. Solution method

For the present study, the equations for the unknown U, V, W, ξ, θ and $\mathrm{d}\bar{P}/\mathrm{d}Z$ are coupled. The coupled governing equations are solved by employing vorticity–velocity method for three-dimensional parabolic flow [25]. The field solutions for a given combination of parameters are calculated by a marching technique based on the DuFort–Rankel scheme [26]. The detailed numerical method and solution procedure can be found in Ref. [27]. In this study, the radiative transfer equation is obtained by the discrete ordinates method with S_N quadrature [28–30]. The solid angle 4π is discretized into a finite number of directions, the discrete ordinate forms of radiative transfer equation is applied at these directions with the integral term replaced by a numerical quadrature and becomes

$$\mu_m\frac{\partial\psi_m}{\partial X}+\eta_m\frac{\partial\psi_m}{\partial Y}+\tau\psi_m=(1-\omega)\tau\theta^4+\frac{\omega\tau}{4\pi}\sum_{m'}w_{m'}^*\phi_{m'm}\psi_m \tag{27}$$

Table 1
Effects of grid size on local Nu_t for $Ra^* = 5 \times 10^4$, $\delta = 100$, $\gamma = 1$, $\theta_o = 0.3$, $N_c = 0.1$, $\varepsilon_w = 0.5$, $\tau = 1.0$, and $\omega = 0$

$M \times N(\Delta Z^*)$	Z^*					
	0.001	0.005	0.01	0.05	0.1	0.3
$81 \times 81(1 \times 10^{-5} \sim 2 \times 10^{-4})$	14.08	8.13	7.15	7.83	6.92	5.86
$51 \times 51(1 \times 10^{-5} \sim 2 \times 10^{-4})$	14.28	8.14	7.17	7.88	6.94	5.86
$51 \times 51(1 \times 10^{-6} \sim 2 \times 10^{-4})$	14.38	8.14	7.17	7.88	6.94	5.86
$31 \times 31(1 \times 10^{-5} \sim 2 \times 10^{-4})$	16.13	8.24	7.22	7.93	6.94	5.86

with associated boundary conditions

$$\psi_m = \varepsilon_w + \frac{1-\varepsilon_w}{\pi}\sum_{m'}\psi_{m'}|\mu_{m'}|w^*_m, \quad \mu_m > 0,\ \mu_{m'} < 0,\ X = 0 \tag{28}$$

$$\psi_m = \varepsilon_w + \frac{1-\varepsilon_w}{\pi}\sum_{m'}\psi_{m'}|\mu_{m'}|w^*_m, \quad \mu_m < 0,\ \mu_{m'} > 0,\ X = \frac{1+\gamma}{2} \tag{29}$$

$$\psi_m = \varepsilon_w + \frac{1-\varepsilon_w}{\pi}\sum_{m'}\psi_{m'}|\eta_{m'}|w^*_m, \quad \eta_m > 0,\ \eta_{m'} < 0,\ Y = 0 \tag{30}$$

$$\psi_m = \varepsilon_w + \frac{1-\varepsilon_w}{\pi}\sum_{m'}\psi_{m'}|\eta_{m'}|w^*_m, \quad \eta_m < 0,\ \eta_{m'} > 0,\ Y = \frac{1+\gamma}{2\gamma} \tag{31}$$

where subscripts m and m' represent the directions of the discrete ordinates and w^*_m are the quadrature weights.

The discrete form of the phase function $\phi_{m'm}$ is expressed as

$$\phi_{m'm} = \sum_{n=0}^{N^*} a_n P_n(\mu_{m'}\mu_m + \eta_{m'}\eta_m + \zeta_{m'}\zeta_m) \tag{32}$$

The integro-differential radiative transfer equation is transformed by the angular discretization into a set of coupled partial differential equations. The choice of the quadrature scheme affects the accuracy of the S_N method, and S_6 scheme is employed so the total number of the discrete direction is 24. The momentum-marching technique [31] is used to calculate the discrete directions and quadrature weights. The dimensionless radiation intensity, radiation flux, and incident radiation are calculated by solving Eqs. (27)–(31) using procedure described by Modest [30].

The grid distributions in the entrance region were arranged to be uniform in the cross-sectional plane but axially non-uniform. A numerical experiment was conducted with various grid distributions in the cross-sectional plane ($M \times N$) and axial step size (ΔZ^*) to check the independence of the grid resolution of the numerical results. There are four grid distributions tested in the analysis and shown in Table 1. They are $31 \times 31(1 \times 10^{-5} \sim 2 \times 10^{-4})$, $51 \times 51(1 \times 10^{-5} \sim 2 \times 10^{-4})$, $51 \times 51(1 \times 10^{-6} \sim 2 \times 10^{-4})$, and $81 \times 81(1 \times 10^{-5} \sim 2 \times 10^{-4})$, respectively. It is found that the deviations in local total Nusselt number Nu_t calculated with 51×51 ($\Delta Z^* = 1 \times 10^{-5} \sim 2 \times 10^{-4}$) and $81 \times 81(1 \times 10^{-5} \sim 2 \times 10^{-4})$ are always less than 2% for the base case of $Ra^* = 5 \times 10^4$, $\delta = 100$, $\gamma = 1$, $N_c = 0.1$, $\varepsilon_w = 0.5$, $\tau = 1$, and $\omega = 0$. Parametrical analysis is conducted by changing one of the parameters. Furthermore, the deviations in Nu_t calculated with $51 \times 51(1 \times 10^{-5} \sim 2 \times 10^{-4})$ and $51 \times 51(1 \times 10^{-6} \sim 2 \times 10^{-4})$ are also less than 2%. Therefore, the computations with grid distribution of $51 \times 51(1 \times 10^{-5} \sim 2 \times 10^{-4})$ are considered to be sufficiently accurate to describe the flow and heat transfer in this study. The local Nusselt number and friction factor were found to agree within 2%. The above program tests indicate that the adopted solution methods are suitable. The resulting data are also compared with those in Ref. [32] for validation.

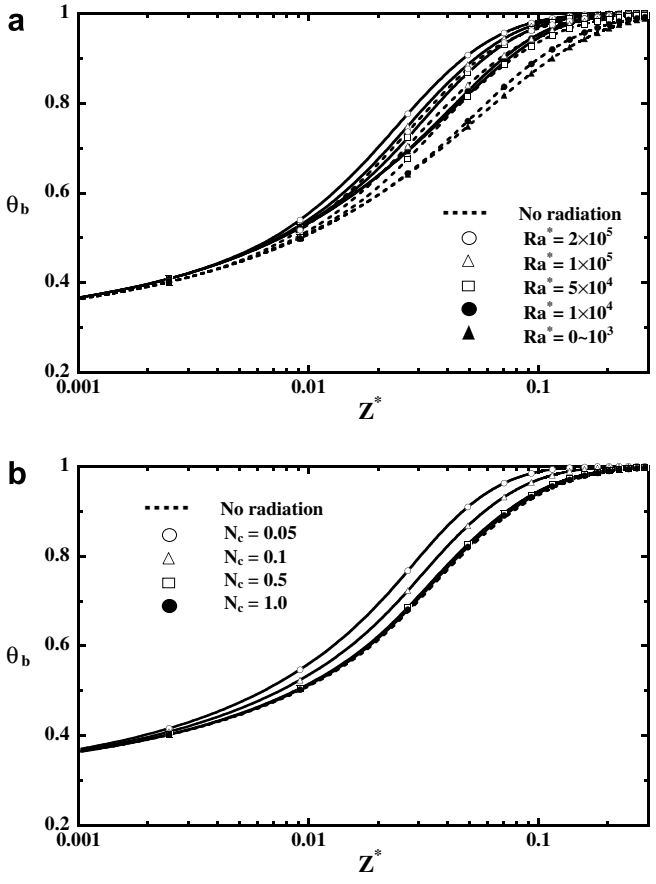

Fig. 2. Effects of (a) Rayleigh number and (b) conduction-to-radiation parameter on the bulk temperature distribution along the axial direction.

4. Results and discussion

In the work, the results for air flowing in a heated rectangular duct over a certain range of governing parameters are presented. Therefore, the Prandtl number is set to be 0.7 and the ratio of air inlet temperature and wall temperature is fixed at $\theta_o = 0.3$. The parameters employed in this analysis include mixed convection parameter ($0 \leqslant \delta \leqslant 200$), modified Rayleigh number ($0 \leqslant Ra \leqslant 2 \times 10^5$), conduction-to-radiation parameter ($0.05 \leqslant N_c \leqslant 1$), aspect ratio ($0.5 \leqslant \gamma \leqslant 2$), optical thickness ($0.1 \leqslant \tau \leqslant 2$), wall emissivity ($0 \leqslant \varepsilon_w \leqslant 1$), and single scattering albedo ($0 \leqslant \omega \leqslant 1$). Numerical solutions were obtained for axial distributions of the bulk temperature, local friction factor fRe, and local total Nusselt number Nu_t.

Fig. 2 shows the axial distributions of the bulk temperature affected by modified Rayleigh number Ra^* and conduction-to-radiation parameter N_c. Results without radiation effect, presented with dashed line, are also sketched for comparison. It is clear that due to the strong buoyancy effect, the bulk temperature develops quickly with larger Ra^*. It is also noted that the effect of radiation on the thermal development is insignificant near the entrance. However, radiation effect tends to equalize the temperature in the flow at the downstream ($Z^* > 0.2$). In addition, the bulk temperature is almost the same as that without radiation when N_c is large ($N_c > 0.5$), corresponding to a weak radiation-convection interaction. The bulk temperature is higher with stronger radiation effect ($N_c = 0.05$) since radiative heat flux is an additional mode of energy transport.

Fig. 3 depicts the effect of mixed convection parameter δ n the axial distributions of the friction factor fRe and the local Nusselt number Nu_t. It is noted that this parameter is proportional to the sinusoidal function of the inclination angle. Thus a higher value of δ means a higher inclination angle for constant Ra^*/Re. The curve of $\delta = 0$ represents the resulting data for a horizontal duct. Fig. 3a indicates that for the same value of Ra^*/Re, the inclination angle significantly increases the local friction factor in the very inlet region. The curves then tend to merge together and suggest that the effect is restricted in the entrance region. Radiation is found to lower the friction factor slightly. On the other hand, Fig. 3b implies that the radiation effect apparently increases the local Nusselt number as well as δ. Observation of these curves reveals that Nusselt number near the inlet declines at first due to forced convection. It then attains a local minimum because the convection effect is balanced by the buoyancy effect. The buoyancy effect then dominates over the entrance convection effect and results in

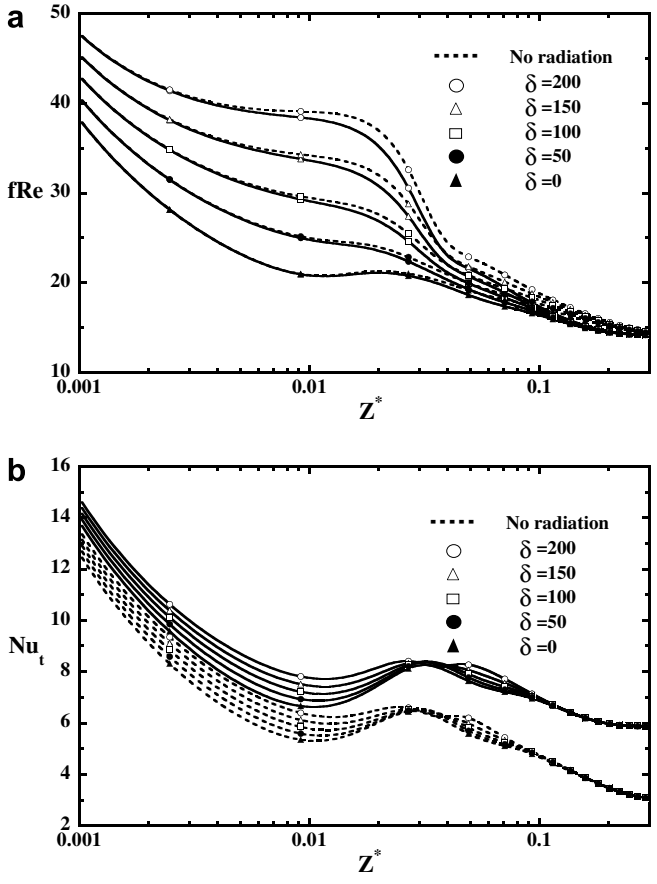

Fig. 3. Effect of mixed convection parameter δ on the local (a) friction factor and (b) Nusselt number for $\gamma = 1$.

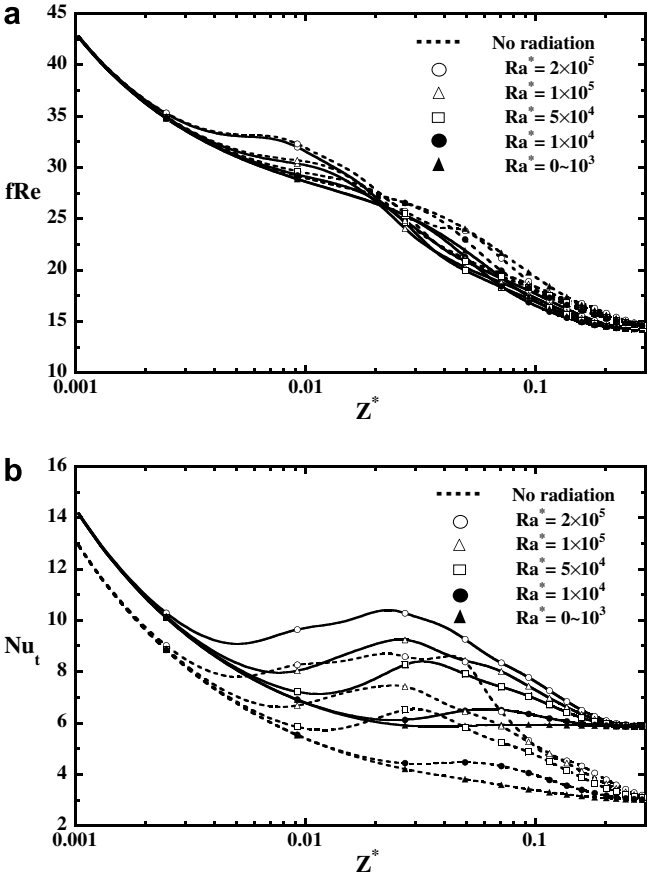

Fig. 4. Effect of Rayleigh number on the local (a) friction factor and (b) Nusselt number for $\gamma = 1.0$.

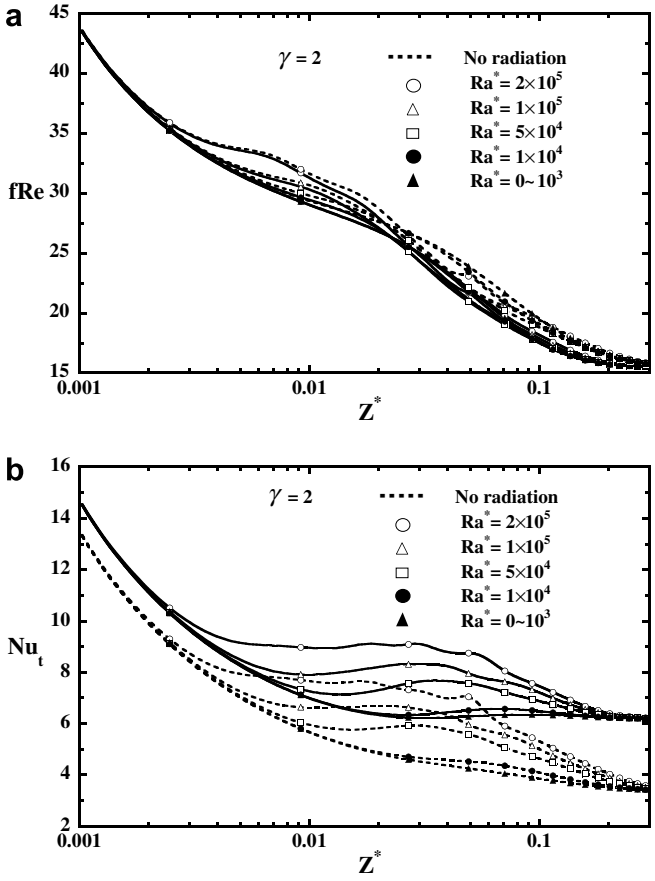

Fig. 5. Effect of Rayleigh number on the local (a) friction factor and (b) Nusselt number for $\gamma = 0.5$.

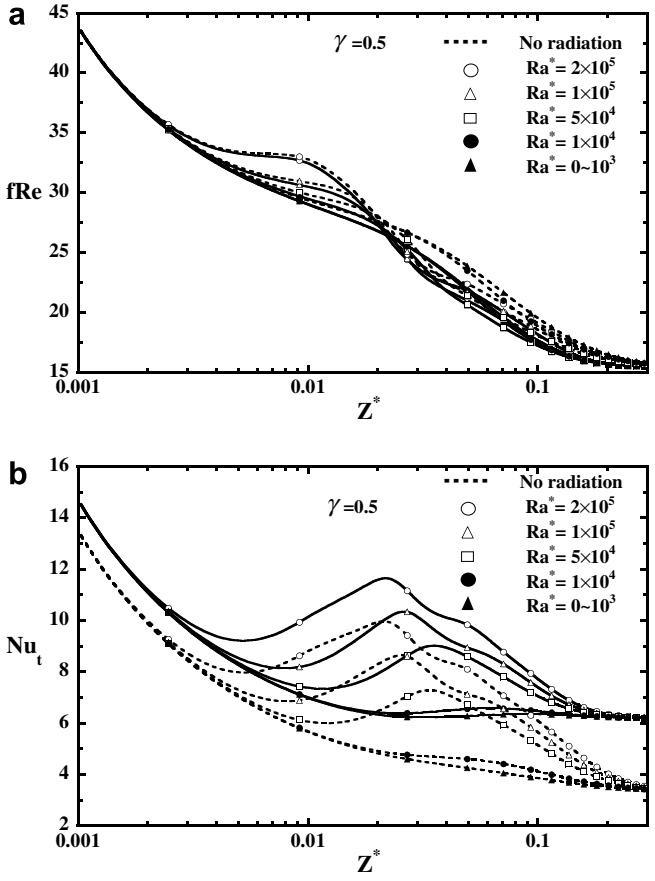

Fig. 6. Effect of Rayleigh number on the local (a) friction factor and (b) Nusselt number for $\gamma = 2$.

a local maximum of Nu_t. Past that location, Nu_t decreases asymptotically corresponding to the full development of bulk temperature. The curves with and without radiation show shift relations and imply that the coupled effect between radiation and inclination angle is weak. It is found that the curves with and without radiation approach to different asymptotic values. It means that the radiation effect give rise to a different thermally fully development states.

Effects of the channel geometry on the friction factor and Nusselt number are of practical interest. Figs. 4–6 present the effects of modified Rayleigh number Ra^* on the axial distributions of the local fRe and Nu_t for $\gamma = 1.0$, 0.5, and 2.0, respectively. Results indicate that friction factor with radiation effect is slightly lower than that without for all the aspect ratio and Ra^* values. Obviously, effects of Ra^* are practically negligible as Ra^* is small ($<10^3$). Higher Ra^* causes more fRe deviation from that for $Ra^* \sim 0$ while the difference takes place in a small inlet region. The figures also show that fRe distribution is almost independent of γ.

As for the axial distributions of Nu_t, it is seen that both Ra^* and radiation effect have significant influence on the total heat transfer. It is also observed that Nu_t decreases in the inlet region due to entrance forced convection and then reaches local minimum since the entrance and buoyancy effects balance out. The buoyancy effects on Nu_t are insignificant up to a certain distance, but have a substantial augmentation at further downstream. Close comparison shows that data of lower γ cause higher Nu_t in the entrance region, meaning the narrow and tall duct causes more significant convective heat transfer. This is due to the fact that a duct with smaller γ results in stronger buoyancy effects than a duct with larger γ does. The value of Ra^* affects the local Nu_t in the entrance region. But the radiation affects the Nu_t through out the duct.

The effects of the conduction-to-radiation parameter N_c on the axial variation of the local fRe and Nu_t are shown in Fig. 7. It is seen that fRe is not apparently influenced by N_c in the very entrance region, since the forced convection is predominant such that the velocity gradient is small in this region. However, the radiation effect becomes more important in the downstream range and causes deviation. It is found that the fRe decreases with decreasing N_c, indicating that friction factor is reduced as radiation effect increases. This may be explained by the fact that the temperature field is flattened with the presence of radiation causing a reduction of buoyancy effect, which in turns leads to the reduction in fRe at the downstream. It is observed in Fig. 7(b) that the local Nu_t with radiation effect is larger than that without radiation effect. This can be easily understood by

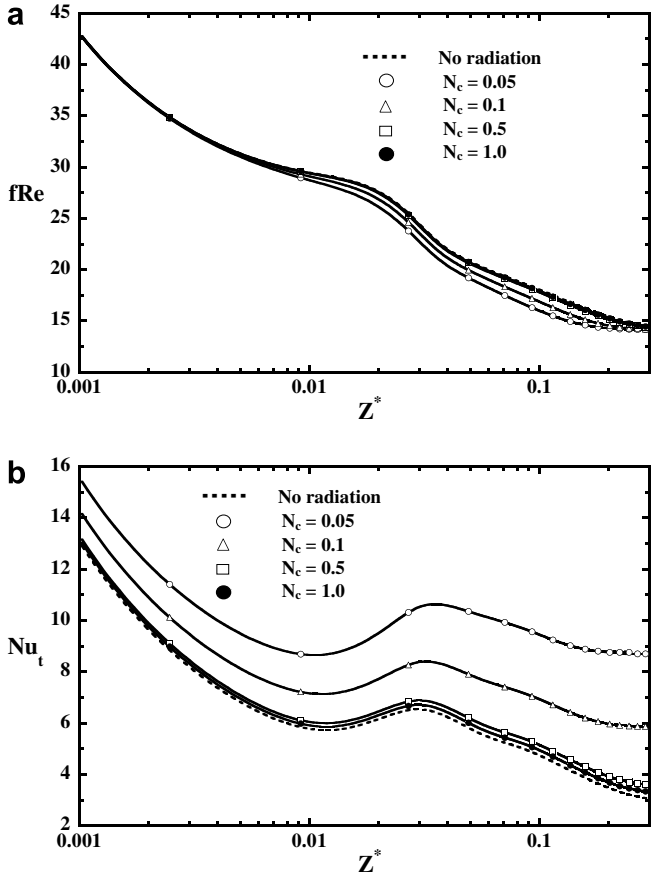

Fig. 7. Effect of conduction-to-radiation parameter on the local (a) friction factor and (b) Nusselt number.

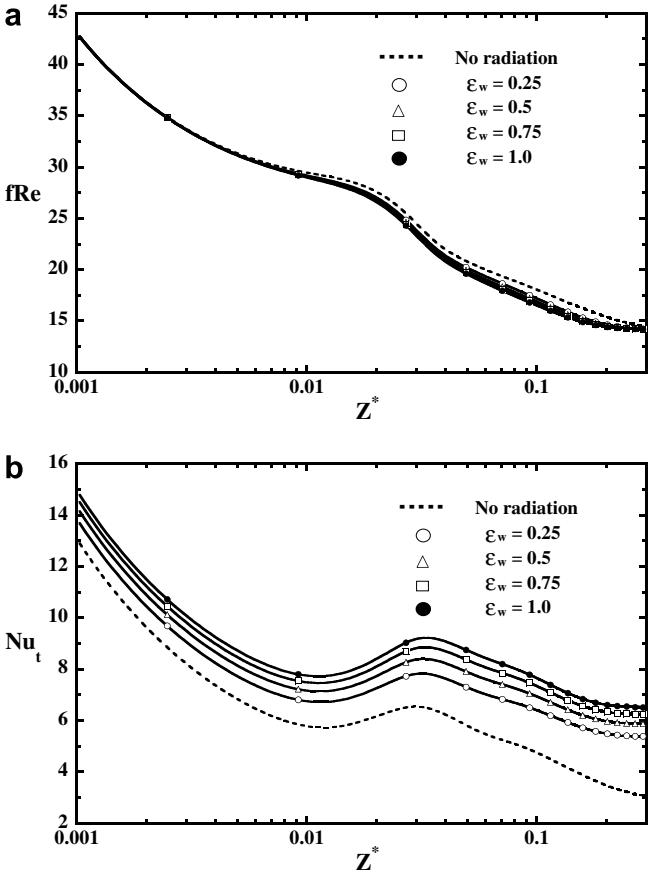

Fig. 8. Effect of wall emissivity on the local (a) friction factor and (b) Nusselt number.

the fact that thermal radiation is an additional mechanism of heat transfer and the radiation source term in the energy equation augments the rate of thermal development as aforementioned. Therefore, the radiation effect enhances both the heat flux through fluid and the rate of thermal development. It is also noted that the Nu_t converges to the case of no radiation with increasing N_c (>0.5), suggesting that effect of radiation is negligible as the N_c is larger than 0.5.

Fig. 8 presents the effects of wall emissivity ε_w on the local fRe and Nu_t . Similarly, it is found in Fig. 8(a) that the effects of $\varepsilon_w$on the fRe are restricted in the downstream region. It is also observed that the stronger radiation effect, the less the value of fRe. Apparently, the local Nu_t with radiation effect is larger than that without. Besides, Nu_t increases as the wall emissivity ε_w increases and the heat transfer is the maximum for a black duct ($\varepsilon_w = 1$).

The optical thickness τ of the medium is an important radiation property in the heat transfer and fluid flow. A small τ indicates medium does not absorb and emit much energy, while a large τ indicates a strongly radiative participating medium. The influence of optical thickness τ on the axial distribution of fRe and Nu_t is depicted in Fig. 9. It is easily seen that the optical thickness does not affect the local fRe in the very inlet. At the downstream near by, fRe decreases as τ increases. The trend of curves is similar to that in Fig. 7. A larger τ indicates a stronger radiation effect. Hence fRe decreases as τ increases. The reason is the same as aforementioned. It is also shown in Fig. 9(b) that the local Nu_t increases with the increase of τ. From the deviation of curves, it is also found that for a system with a larger τ, the radiation has a stronger effect on Nu_t. Therefore, it is concluded that more heat is transferred from a medium with a higher τ than that with a lower τ.

In many physical applications particulates are present in the fluid. Therefore, scattering processes are also important in radiative heat transfer. The effects of the single scattering albedo on the fluid flow and heat transfer are of interest. In this study, the scattering is assumed to be isotropic. Fig. 10 shows the effects of single scattering albedo ω on the axial variations of local fRe and Nu_t. The amount of energy that impinges upon the gray medium depends on the scattering albedo. When single scattering albedo ω approaches zero, the emission and absorption of the radiative energy within the medium dominate. But as the scattering albedo ω approaches unity, the scattering of the radiative heat transfer dominates. It is seen that the local fRe is slightly raised when ω is varied from 1.0 to 0. In addition, the local Nu_t decreases with increasing ω. Observation on Figs. 4–10 indicates that radiation properties affect local fRe in the entrance region, while they affect the Nu_t through out the

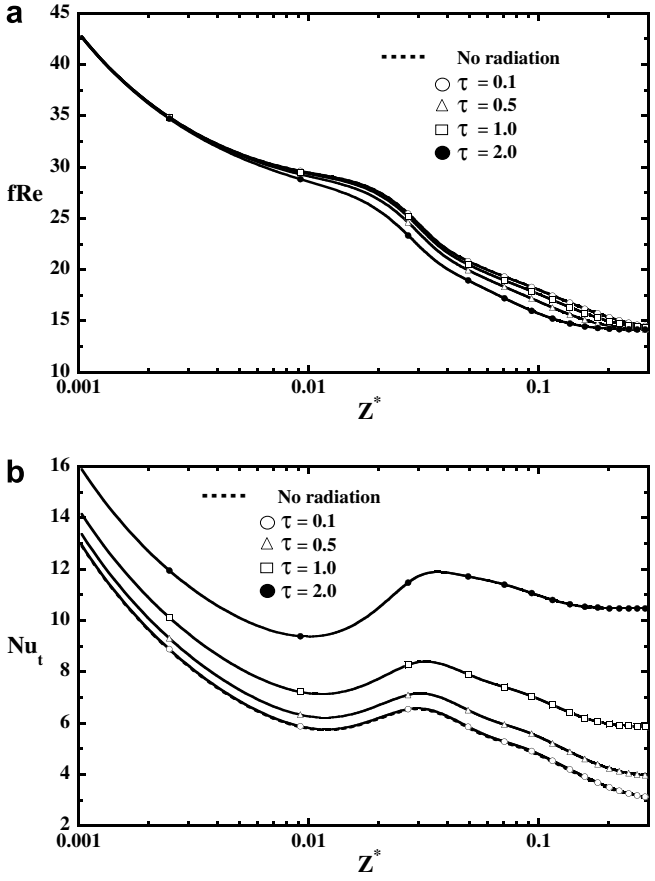

Fig. 9. Effect of optical thickness on the local (a) friction factor and (b) Nusselt number.

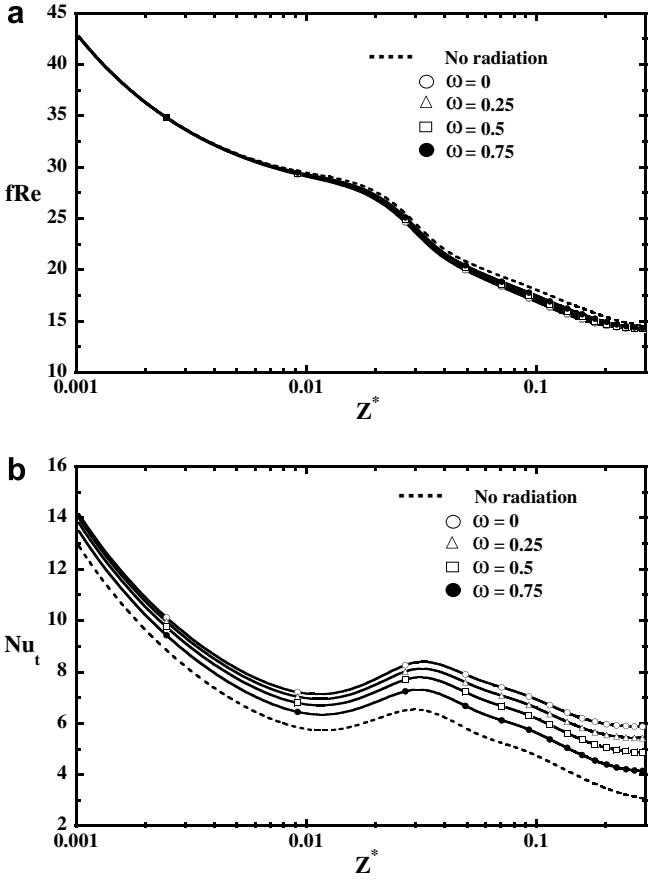

Fig. 10. Effect of single scattering albedo on the local (a) friction factor and (b) Nusselt number.

ducts. The inclination angle is found to show more significant effect on local *fRe* than radiation properties due to buoyancy.

5. Conclusions

The study of radiation effects on mixed convection in inclined rectangular ducts has been performed numerically. The effects of modified Rayleigh number, aspect ratio γ of the duct, conduction-to-radiation parameter N_c, optical thickness, wall emissivity, and single scattering albedo on momentum, heat and mass transfer have been analyzed in detail. Brief summaries of the major results are listed below:

1. Both buoyancy and radiation effects enhance thermal development and cause higher bulk temperature in the entrance region. Radiative heat flux is an additional mode of energy transport and the local total Nusselt number is augmented by the radiation effect.
2. The inclination angle enhances both the local friction factor and local Nusselt number. But the effect is restricted in the entrance region only.
3. Results show that Nu_t slightly increases as γ decreases for same Ra^*.
4. Buoyancy shows much stronger effect on the local friction factor than other parameters mentioned in this study. Both the local friction factor and total Nusselt number are increased by buoyancy.
5. The local total Nusselt number is increased by increasing optical thickness of the gray medium, wall emisivity and reducing single scattering albedo.

Acknowledgements

The authors acknowledge the financial support of the present work by the National Science Council, R.O.C. through the contract NSC93-2212-E211-011. The support from Technology and Science Institute of Northern Taiwan is also acknowledged.

References

[1] E. Sediki, A. Soufiani, M.S. Sifaoui, Combined gas radiation and laminar mixed convection invertical circular tubes, Int. J. Heat Fluid Flow 24 (2003) 736–746.

[2] M. Hishida, Y. Nagano, M.S. Montesclaros, Combined forced and free convection in the entrance region of an isothermally heated horizontal pipe, J. Heat Transfer 104 (1982) 153–159.

[3] R. Echigo, S. Hasegawa, K. Kamiuto, Composite heat transfer in a pipe with thermal radiation of two-dimensional propagation in connection with the temperature rise in a flowing medium upstream of a heating section, Int. J. Heat Mass Transfer 18 (1975) 1149–1159.
[4] A.T. Wassel, D.K. Edwards, Molecular gas radiation in a laminar or turbulent pipe flow, ASME J. Heat Transfer 98 (1976) 101–107.
[5] F.H. Azad, M.F. Modest, Combined radiation and convection in absorbing emitting and anisotropically scattering gas-particulate tube flow, Int. J. Heat Mass Transfer 24 (1981) 1681–1697.
[6] T. Seo, D.A. Kaminski, M.K. Jensen, Combined convection and radiation in simultaneously developing flow and heat transfer with nongray gas mixtures, Numer. Heat Transfer Part A 26 (1994) 49–66.
[7] L.K. Yang, Combined mixed convection and radiation in a vertical pipe, Int. Commun. Heat Mass Transfer 18 (1991) 419–430.
[8] L.K. Yang, Forced convection in a vertical pipe with combined buoyancy and radiation effects, Int. Commun. Heat Mass Transfer 19 (1992) 249–262.
[9] W.M. Yan, H.Y. Li, D. Lin, Mixed convection heat transfer in a radially rotating square duct with radiation effects, Int. J. Heat Mass Transfer 42 (1999) 35–47.
[10] W.M. Yan, H.Y. Li, Radiation effects on mixed convection heat transfer in a vertical square duct, Int. J. Heat Mass Transfer 44 (2001) 1401–1410.
[11] A. Raptis, Flow of a micropolar fluid past a continuously moving plate by the presence of radiation, Int. J. Heat Mass Transfer 41 (1998) 2865–2866.
[12] Y.J. Kim, A.G. Fedorov, Transient mixed radiative convection flow of a micropolar fluid past a moving, semi-infinite vertical porous plate, Int. J. Heat Mass Transfer 46 (2003) 1751–1758.
[13] P. Talukdar, S.C. Mishra, D. Trimis, F. Durst, Combined radiation and convection heat transfer in a porous channel bounded by isothermal parallel plates, Int. J. Heat Mass Transfer 47 (2004) 1001–1013.
[14] T.W. Tong, S.B. Sathe, Heat transfer characteristics of porous radiant burners, J. Heat Transfer 113 (1991) 423–428.
[15] C. Debbissi, J. Orfi, S. Ben Nasrallah, Evaporation of water by free convection in a vertical channel including effects of wall radiative properties, Int. J. Heat Mass Transfer 44 (2001) 811–826.
[16] E. Sediki, A. Soufiani, M.S. Sifaoui, Combined gas radiation and laminar mixed convection in vertical circular tubes, Int. J. Heat Fluid flow 24 (2003) 736–746.
[17] H.V. Mahaney, F.P. Incropera, S. Ramadhyani, Development of laminar mixed convection flow in a horizontal rectangular duct with uniform bottom heating, Numer. Heat Transfer 12 (1987) 137–155.
[18] M. Wang, T. Tsuji, Y. Nagano, Mixed convection with flow reversal in the thermal entrance region of horizontal and vertical pipes, Int. J. Heat Mass Transfer 37 (1994) 2305–2319.
[19] W.M. Yan, Turbulent mixed convection heat and mass transfer in a wetted channel, ASME J. Heat Transfer 117 (1995) 229–233.
[20] Z.A. Hammou, B. Benhamou, N. Galanis, J. Orfi, Laminar mixed convection of humid air in a vertical channel with evaporation or condensation at the wall, Int. J. Thermal Sci. 43 (2004) 531–539.
[21] C.C. Huang, W.M. Yan, J.H. Jang, Laminar mixed convection heat and mass transfer in vertical rectangular ducts with film evaporation and condensation, Int. J. Heat Mass Transfer 48 (2005) 1772–1784.
[22] J.H. Jang, W.M. Yan, C.C. Huang, Mixed convection heat transfer enhancement through film evaporation in inclined square ducts, Int. J. Heat Mass Transfer 48 (2005) 2117–2125.
[23] J.N. Lin, F.C. Chou, W.M. Yan, P.Y. Tzeng, Combined buoyancy effects of thermal and mass diffusion on laminar forced convection in the thermal entrance region of horizontal square channels, Can. J. Chem. Eng. 79 (1992) 681–689.
[24] C.C. Huang, T.F. Lin, Numerical simulation of transitional aiding mixed convection air flow in a bottom heated inclined rectangular duct, Int. J. Heat Mass Transfer 39 (1996) 1697–1710.
[25] K. Ramakrishna, S.G. Rubin, P.K. Khosla, Laminar natural convection along vertical square ducts, Numer. Heat Transfer 5 (1982) 59–79.
[26] P.J. Roche, Computational Fluid Dynamics, Reinhold, New York, 1971, pp. 61–64.
[27] W.M. Yan, C.Y. Soong, Simultaneously developing mixed convection in radially rotating rectangular ducts, Int. J. Heat Mass Transfer 38 (1995) 665–677.
[28] W.A. Fiveland, Three-dimensional radiative heat transfer solutions by the discrete-ordinates method, J. Thermophys. Heat Transfer 2 (1988) 309–316.
[29] T.Y. Kim, S.W. Bake, Analysis of combined conductive and radiative heat transfer in a two-dimensional rectangular enclosure using the discrete ordinates method, Int. J. Heat Mass Transfer 34 (1991) 2265–2273.
[30] M.F. Modest, Radiative Heat Transfer, McGraw-Hill, New York, 1993, pp. 541-571.
[31] B.G. Carlson, K.D. Lathrop, Transport theory: the method of discrete ordinates, in: H. Greenspan, C.N. Kelber, D. Okrent (Eds.), Computing Methods in Reactor Physics, Gordon & Breach, New York, 1968, pp. 165–266.
[32] H.C. Chiu, J.H. Jang, W.M. Yan, Mixed convection heat transfer in horizontal rectangular ducts with radiation effects, Int. J. Heat Mass Transfer 50 (2007) 2874–2882.